Available online at www.sciencedirect.com
SCIENCE DIRECT
Journal of Sound and Vibration 265 (2003) 507–525
JOURNAL OF SOUND AND VIBRATION
www.elsevier.com/locate/jsvi

Simulating non-linear coupled oscillators by an iterative differential quadrature method

S. Tomasiello*

DiSGG, Faculty of Engineering, University of Basilicata, C.da Macchia Romana, 85100 Potenza, Italy

Received 3 April 2002; accepted 16 July 2002

Abstract

An iterative method based on differential quadrature rules is proposed as a new unified frame of resolution for non-linear two-degree-of-freedom systems. Dynamical systems with Duffing-type non-linearity have been considered. Differential quadrature rules have been applied with a careful distribution of sampling points to reduce the governing equation of motion to two second-order non-linear, non-autonomous ordinary differential equations and to solve the time-domain problem. The time domain of the problem is discretized by means of time intervals, with the same distribution of sampling points used to discretize the space domain (which can be seen as a single interval). It will be shown that accurate solutions depend not only on the choice of the distribution of sampling points, but also on the length of the time interval one refers to in the computations. The numerical results, utilized to draw Poincaré maps, are successfully compared with those obtained using the Runge–Kutta method.

1. Introduction

The normal way to proceed to study non-linear continuous systems is to operate a discretization in space and to compute the time-dependent solution numerically.

Discretization essentially transforms vibration problems described by partial differential equations into problems described by sets of simultaneous ordinary differential equations. The two main classes of discretization procedures are based on the expansion of the solution in a finite series of given functions. These classes are referred to as Rayleigh–Ritz-type methods and weighted residual methods. In the first class one can include the finite element method, although

*Tel.: +39 (0) 971-205-102; fax: +39 (0) 971-205-070.
E-mail address: tomasiello@unibas.it (S. Tomasiello).

0022-460X/03/$ - see front matter © 2002 Elsevier Ltd. All rights reserved.
doi:10.1016/S0022-460X(02)01525-0

the procedural details differ from those of the classical Rayleigh–Ritz method. The second class includes perhaps the most widely used discretization method, namely, the Galerkin method.

The Ritz–Galerkin techniques need to determine eigenfunctions and this can be difficult. To overcome this problem, differential quadrature rules with a suitable distribution of sampling points have been applied to reduce non-linear boundary–initial-value problems to a system of coupled non-linear ordinary differential equations [1].

The method illustrated in Ref. [1] is based on a new rule to generate sampling points which allows, using only six points, the discretization errors to be minimized.

A way to improve this method seems to be to discretize the whole space-time domain by means of differential quadrature rules with the same distribution of sampling points.

This is possible by specifying the two parameters governing the rule mentioned above and by repeating the procedure on the time axis with a simple co-ordinates translation, by a quantity equal to the length of the time interval one refers to in discretizing the time domain. In fact, solutions may be calculated over a rectangular quadrature grid which has N points in the space direction and $(M \times N)$ in the time direction, where N is the number of sampling points (here limited to six) and M fixes the upper limit of the range over which the numerical solution is sought, so it may change each time.

The resulting method, referred to here as the iterative differential quadrature (IDQ) method, has been successfully used to simulate two non-linear oscillators coupled in linear terms, by showing some aspects of the system behaviour.

More attention has recently been given to the behaviour of non-linear coupled oscillators. Papers devoted to the analysis of these systems mainly use a semi-analytical approach [2,3]. Numerical investigations can be found in Ref. [4].

The literature has several examples of the applications of differential quadrature rules, although in different versions, to discretize either the space domain or the time domain.

A good review of the various applications of the method is offered in Ref. [5]. This paper [5], among other things, suggests the use of the Frechet derivative to treat non-linearity. This concept, together with that of generalized differential quadrature rules [6–9], inspired a recent study, which considered a single Duffing oscillator [10].

2. The differential quadrature method: a brief overview

The basic idea of the differential quadrature method is that the derivative of a function with respect to a space variable at a given point can be approximated as a weighted linear sum of the function values at all discrete points in the domain of that variable. In terms of dimensionless variables, it is assumed that, at a point $\zeta = \zeta_i$, the rth order derivative of a function $w(\zeta)$, defined in the domain $(0, 1)$ with N discrete grid points, is given by

$$\left[\frac{\mathrm{d}^r w}{\mathrm{d}\zeta^r}\right]_{\zeta=\zeta_i} = \sum_{j=1}^{N} A_{ij}^{(r)} w_j, \quad i = 1, 2, \ldots, N, \tag{1}$$

where $A_{ij}^{(r)}$ are the weighting coefficients of the rth order derivative.

The weighting coefficients are determined by substituting approximating functions to the originary function $w(\zeta)$ in Eq. (1). In the generalized differential quadrature (GDQ) method [8] these test functions are assumed to be the Lagrange interpolated polynomial. The off-diagonal terms of the weighting coefficient matrix of the first order derivative become:

$$A_{ij}^{(1)} = \frac{\prod_{v=1, v\neq i}^{N}(\zeta_i - \zeta_v)}{(\zeta_i - \zeta_j)\prod_{v=1, v\neq j}^{N}(\zeta_j - \zeta_v)}, \quad i,j = 1,2,\ldots,N, \; j\neq i. \tag{2}$$

The off-diagonal terms of the weighting coefficient matrix of the higher order derivative are obtained through the recurrence relationship:

$$A_{ij}^{(r)} = r\left[A_{ii}^{(r-1)}A_{ij}^{(1)} - \frac{A_{ij}^{(r-1)}}{(\zeta_i - \zeta_j)}\right], \quad i,j = 1,2,\ldots,N, \quad j\neq i, \tag{3}$$

where $2 \leqslant r \leqslant (N-1)$.

The diagonal terms of the weighting coefficient matrix are given by

$$A_{ii}^{(r)} = -\sum_{\substack{v=1\\ v\neq i}}^{N} A_{iv}^{(r)}, \quad i = 1,2,\ldots,N, \tag{4}$$

where $1 \leqslant r \leqslant (N-1)$.

Assuming the Lagrange interpolated polynomial as test functions, there is no restriction in the choice of the grid co-ordinates. So, in order to have more accurate solutions, it is possible to generate the sampling points as follows:

$$\zeta_i = \frac{1}{2}\left[1 - \cos\frac{(i-1)}{(N-1)}\pi\right], \quad i = 1,2,\ldots,N. \tag{5}$$

In order to overcome the problem of the δ-points [5], Shu and Du [11] support the GDQ method with a direct substitution of the boundary conditions into the governing equation.

3. The iterative differential quadrature method

The IDQ method moves away from the Shu and Du concept, but uses grid co-ordinates which are different from those given by Eq. (5). In fact, the IDQ method is based on a particular rule generating a distribution of sampling points which give sufficiently accurate results [1].

This rule is given below as

$$\zeta_i = \left(\frac{i-1}{N-1}\right)^{Nb_i/i\sqrt{i}}, \tag{6}$$

where b_i are unknown coefficients to be fixed.

Because of the symmetry of the sampling points distribution, with $N = 6$, only b_2 and b_3 need to be fixed.

It has already been shown that the results in the space domain are influenced by b_3 and not by b_2 in the linear range or not significantly in the non-linear range by the same coefficient [1]. It has also been shown that the results are in good agreement for values of b_3 (close to 1.2). Instead, the coefficient b_2 influences the solution in the time domain, as will be seen in the following sections. The concept of IDQ method is to use the same sampling points distribution to discretize the whole space–time domain.

On the spatial axis the interval $0 \leqslant \zeta_i \leqslant 1$ is considered by scaling the dimensional spatial co-ordinate with the length of the problem domain. The time axis can similarly be regarded as an unitary dimensionless intervals series, where each interval is the result of a time-scaling operation from an interval $\Delta\tau$ of suitable length. In particular, for free dynamical systems the natural period can be considered, whereas for forced dynamical systems one can consider the forcing term period. In order to have more accurate results, a solution is calculated for a fraction of the period referred to. In particular, by assuming 4 as denominator of the above-mentioned fraction and by setting $b_2 = 1.4$, as well as setting $b_3 = 1.2$, one obtains sufficiently accurate results, as it will be shown later. The solution is calculated for each of the M time intervals with the following change in the time variable τ:

$$\bar{\tau}^{[i]} = \frac{\tau - \sum_{k=1}^{i-1} \Delta\tau_k}{\Delta\tau_i}, \quad i = 1, 2, \ldots, M \tag{7}$$

and with the initial conditions:

$$w_{l1}^{[i]} = w_{lN}^{[i-1]}, \qquad \dot{w}_{l1}^{[i]} = \dot{w}_{lN}^{[i-1]}, \quad i = 1, 2, \ldots, M, \;\; l = 1, 2,$$

where i is referred to the ith time interval, l indicates the oscillator referred to, w is the displacement, and $\dot{w}$ is the velocity. In order to indicate the values referred to the ith time interval, squared bracket symbolism has been adopted. The choice of the number of intervals M depends on the kind of solution required but in any case, the sampling points distribution for each time interval is equal to the distribution applied to the spatial interval.

In this paper, solutions obtained with the IDQ method are used to draw Poincaré maps, so the number M changes according to circumstances.

The distribution resulting from the cited values of b_2 and b_3 is

$$\{0, \quad 0.008, \quad 0.281, \quad 0.719, \quad 0.992, \quad 1\}. \tag{8}$$

4. The model

Consider a simply supported beam with span L, Young's modulus E, moment of inertia I, mass per unit lenght m, and cross-sectional area A, which rests on an hardening non-linear elastic foundation and which is subjected to a compressive load P and to an exciting transverse force $F(z,t) = F(z)\cos\bar{\omega}t$. The foundation is supposed to be defined by the following load–displacement relationship: $q(z) = k_1 v(z) + k_3 v(z)^3$, where $q(z)$ is the force per unit length, k_1 is the linear Winkler foundation stiffness and $k_3 > 0$ is the hardening non-linear elastic foundation stiffness.

If the beam is considered to be slender, the equation of motion can be written as

$$m\frac{\partial^2 v}{\partial t^2} + EI\frac{\partial^4 v}{\partial z^4} + P\frac{\partial^2 v}{\partial z^2} + k_1 v + k_3 v^3 = F(z)\cos\bar{\omega}t. \tag{9}$$

Eq. (8) can be conveniently written in terms of dimensionless variables as

$$\frac{\partial^2 w}{\partial \tau^2}+\frac{\partial^4 w}{\partial \zeta^4}+\sigma\frac{\partial^2 w}{\partial \zeta^2}+\theta_1 w+\theta_3 w^3=f(\zeta)\cos\omega\tau, \tag{10}$$

where

$$w=\frac{v}{L},\quad \zeta=\frac{z}{L},\quad \tau=\sqrt{\frac{EI}{m}}\frac{t}{L^2},\quad \omega=\sqrt{\frac{m}{EI}}L^2\bar{\omega},$$

$$\sigma=\frac{PL^2}{EI},\quad \theta_1=\frac{k_1L^4}{EI},\quad \theta_3=\frac{k_3L^6}{EI},\quad f(\zeta)=\frac{F(\zeta)L^3}{EI}.$$

The differential quadrature analogue of Eq. (9) for the ith time interval may be written, using the quadrature rules in the ζ and τ co-ordinates and Eq. (7), as

$$\alpha_i^2\sum_{j=1}^{N}A_{kj}^{(2)}w_{lj}+\sum_{j=1}^{2}R_{lj}w_{jk}+\theta_3 w_{lk}^3=f_{lk}\cos\omega\left(\bar{\tau}\Delta\tau_i+\sum_{k=1}^{i-1}\Delta\tau_k\right),$$
$$l=1,2,\;\; k=1,\ldots,N, \tag{11}$$

where N is the number of the sampling points, i.e., six, and

$$\alpha_i=\frac{1}{\Delta\tau_i},\quad f_{lk}=f(\zeta_l,\bar{\tau}_k),$$

$$R_{lj}=L_{(l+2)(j+2)}-\frac{E_{j+2}}{D}L_{(l+2)2}-\frac{H_{j+2}}{G}L_{(l+2)(N-1)}+\theta_1\delta_{lj},$$

with δ_{lj} being equal to the Kronecker operator and

$$L_{lj}=A_{lj}^{(4)}+\sigma A_{lj}^{(2)},$$

$$D=A_{N2}^{(p)}-\frac{A_{N(N-1)}^{(p)}}{A_{1(N-1)}^{(q)}}A_{12}^{(q)},\qquad E_j=A_{Nj}^{(p)}-\frac{A_{N(N-1)}^{(p)}}{A_{1(N-1)}^{(q)}}A_{1j}^{(q)},$$

$$G=A_{N(N-1)}^{(p)}-\frac{A_{N2}^{(p)}}{A_{12}^{(q)}}A_{1(N-1)}^{(q)},\qquad H_j=A_{Nj}^{(p)}-\frac{A_{N2}^{(p)}}{A_{12}^{(q)}}A_{1j}^{(q)}.$$

In the equations above, the quantities p and q depend on external constraints: for a simply supported beam $p=q=2$.

In Eq. (11), the apex [i] has been omitted for simplicity. For more details about the deduction of R_{lj} and the other related quantities, refer to Ref. [1].

The first interval has the following initial conditions:

$$w_{l1}^{[1]}=a,\quad \alpha_1\dot{w}_{l1}^{[1]}=b,\quad l=1,2, \tag{12}$$

where a and b are real numbers.

The second part of Eq. (12) can be written as

$$\alpha_1 \sum_{j=1}^{N} A_{1j}^{(1)} w_{lj}^{[1]} = b, \quad l = 1, 2.$$

This equation can be used in order to obtain $w_{lN}^{[1]}$:

$$w_{lN}^{[1]} = \frac{C_l}{A_{1N}^{(1)}}, \quad l = 1, 2,$$

where

$$C_l = \frac{b}{\alpha_1} - (A_{11}^{(1)} a + \cdots + A_{1(N-1)}^{(1)} w_{l(N-1)}^{[1]}).$$

Finally, $w_{l1}^{[1]}$ and $w_{lN}^{[1]}$ can be substituted into Eq. (11), giving

$$\alpha_1^2 \left(A_{k1}^{(2)} a + \frac{A_{kN}^{(2)} C_l}{A_{1N}^{(1)}} + \sum_{j=2}^{N-1} A_{kj}^{(2)} w_{lj} \right) + \sum_{j=1}^{2} R_{lj} w_{jk} + \theta_3 w_{lk}^3 = f_{lk} \cos \omega \left(\bar{\tau} \Delta\tau_i + \sum_{k=1}^{i-1} \Delta\tau_k \right),$$
$$l = 1, 2, \;\; k = 2, \ldots, N-1. \tag{13}$$

Eq. (13) is also valid for the ith time interval with

$$a = w_{lN}^{[i-1]}, \quad b = \dot{w}_{lN}^{[i-1]}, \quad l = 1, 2$$

and replacing α_1 with α_i.

As can be seen, for each time interval a set of $2 \times (N-2)$ non-linear equations coupled in the linear part is obtained. These equations will be solved with Newton's method.

5. Some numerical results

The solutions obtained by using the IDQ method are compared with the results obtained by applying the Runge–Kutta method to the equation resulting from the only spatial discretization:

$$\ddot{w}_i + \sum_{j=1}^{2} R_{ij} w_j + \theta_3 w_i^3 = f_i \cos \omega\tau, \quad i = 1, 2. \tag{14}$$

For an initial check of the method, solutions have been calculated by assuming $\sigma = 0.1$, $\theta_1 = \theta_3 = 1$ and f as constant, i.e., $f_i = f$. The cases $f = 0$, 1, 10, 100 have been considered, by varying initial conditions. In addition, fundamental resonance with $\omega \approx \omega_{10}$ has been considered.

The cases considered can be classified into three categories. The first one includes cases with a and b which are not equal to zero. Cases belonging to the second category are characterized by having either a or b equal to zero. Finally, the third category includes cases where a and b have the same value.

Computations for each time interval have been carried out by assuming $\Delta\tau = T/4$, where T is the period of the forcing term or the natural period of the first oscillator for the forced or free problem respectively. Tables 1–16 show results obtained for nT with $n = 1, \ldots, 10$.

For brevity, only results obtained for $f = 0$ and 100 have been tabulated.

Table 1
Numerical results for $a=0.5,\ b=1,\ f=0$

n	w_{RK}	w_{IDQ}	Δ%	$\dot{w}_{RK}$	$\dot{w}_{IDQ}$	Δ%
1	0.500625	0.50058	0.008989	0.969191	0.96993	−0.076249
2	0.501231	0.501142	0.017756	0.938345	0.939826	−0.157831
3	0.501818	0.501686	0.026304	0.907459	0.909689	−0.245741
4	0.502385	0.502212	0.034436	0.876535	0.879518	−0.340317
5	0.502933	0.502721	0.042153	0.845579	0.849317	−0.442064
6	0.503462	0.503212	0.049656	0.814582	0.819085	−0.552799
7	0.503972	0.503685	0.056948	0.78355	0.788825	−0.673218
8	0.504462	0.50414	0.06383	0.752478	0.758536	−0.805073
9	0.504933	0.504577	0.070504	0.721371	0.72822	−0.949442
10	0.505385	0.504996	0.076971	0.69024	0.697878	−1.106572

Table 2
Numerical results for $a=0.5,\ b=1,\ f=100$

n	w_{RK}	w_{IDQ}	Δ%	$\dot{w}_{RK}$	$\dot{w}_{IDQ}$	Δ%
1	0.679567	0.680901	−0.196301	32.4329	32.423753	0.028203
2	2.85349	2.87644	−0.804278	57.7146	57.805109	−0.156822
3	7.28859	7.2743	0.196060	30.362	30.602708	−0.792794
4	5.96274	5.98143	−0.313447	−50.5426	−50.880454	−0.668454
5	1.75636	1.76409	−0.440115	−51.4845	−51.451806	0.063503
6	0.532588	0.534046	−0.273758	−22.124	−22.053394	0.319138
7	0.497986	0.499729	−0.350010	9.43368	9.496773	−0.668806
8	0.950073	0.958351	−0.871301	40.5317	40.581247	−0.122243
9	4.00945	4.05298	−1.085685	59.1285	59.283336	−0.261864
10	7.79885	7.757255	0.533348	6.54837	6.347417	3.068748

Table 3
Numerical results for $a=1,\ b=0.5,\ f=0$

n	w_{RK}	w_{IDQ}	Δ%	$\dot{w}_{RK}$	$\dot{w}_{IDQ}$	Δ%
1	1.00093	1.00088	0.004995	0.261435	0.261565	−0.049726
2	1.0013	1.00121	0.008988	0.02268	0.022982	−1.331570
3	1.00109	1.000987	0.010289	−0.216121	−0.215613	0.235054
4	1.00032	1.00021	0.010996	−0.454873	−0.454087	0.172795
5	0.99897	0.998887	0.008309	−0.693369	−0.692306	0.153309
6	0.997053	0.99701	0.004313	−0.93144	−0.930135	0.140106
7	0.994569	0.994584	−0.001508	−1.169	−1.16744	0.133447
8	0.991518	0.991608	−0.009077	−1.40591	−1.40409	0.129454
9	0.9879	0.988084	−0.018625	−1.64205	−1.63994	0.128498
10	0.983718	0.984012	−0.029887	−1.87728	−1.87487	0.128377

Table 4
Numerical results for $a = 1,\ b = 0.5,\ f = 100$

n	w_{RK}	w_{IDQ}	Δ%	$\dot{w}_{RK}$	$\dot{w}_{IDQ}$	Δ%
1	1.17796	1.17913	−0.099324	31.4459	31.4478	−0.006042
2	3.21269	3.23266	−0.621597	54.5955	54.732	−0.250021
3	7.19082	7.17131	0.271318	27.4255	27.7001	−1.001258
4	6.0017	6.02071	−0.316744	−46.6309	−46.9037	−0.585020
5	2.18251	2.19509	−0.576401	−49.1293	−49.1876	−0.118666
6	1.03381	1.03567	−0.179917	−21.2805	−21.2843	−0.017857
7	0.999493	1.00114	−0.164784	10.0516	10.0435	0.080584
8	1.48554	1.49073	−0.349368	40.1622	40.1681	−0.014690
9	4.42628	4.45372	−0.619934	55.0921	55.3048	−0.386081
10	7.64701	7.60511	0.547927	2.50002	2.56432	−2.571979

Table 5
Numerical results for $a = 1,\ b = 0,\ f = 0$

n	w_{RK}	w_{IDQ}	Δ%	$\dot{w}_{RK}$	$\dot{w}_{IDQ}$	Δ%
1	0.99974	0.999726	0.001400	−0.237832	−0.237717	0.048353
2	0.998916	0.998903	0.001301	−0.475584	−0.475301	0.059506
3	0.997525	0.997533	−0.000802	−0.713099	−0.712619	0.067312
4	0.995568	0.995615	−0.004721	−0.950262	−0.949538	0.076190
5	0.993045	0.993151	−0.010674	−1.18685	−1.18592	0.078359
6	0.98996	0.99014	−0.018183	−1.42276	−1.42165	0.078017
7	0.986314	0.986585	−0.027476	−1.65789	−1.65657	0.079619
8	0.982108	0.982486	−0.038489	−1.8921	−1.89056	0.081391
9	0.977343	0.977845	−0.051364	−2.12526	−2.1235	0.082813
10	0.972024	0.972664	−0.065842	−2.35718	−2.35523	0.082726

Table 6
Numerical results for $a = 1,\ b = 0,\ f = 100$

n	w_{RK}	w_{IDQ}	Δ%	$\dot{w}_{RK}$	$\dot{w}_{IDQ}$	Δ%
1	1.16728	1.16837	−0.093379	30.9745	30.9759	−0.004520
2	3.15584	3.17531	−0.616951	54.4315	54.564	−0.243425
3	7.14788	7.13024	0.246786	28.5709	28.8522	−0.984568
4	6.06793	6.08565	−0.292027	−45.9758	−46.2501	−0.596618
5	2.22287	2.23574	−0.578981	−49.4653	−49.5277	−0.126149
6	1.03754	1.03925	−0.164813	−21.7685	−21.773	−0.020672
7	0.999406	1.00087	−0.146487	9.55419	9.54564	0.089490
8	1.464	1.4688	−0.327869	39.7255	39.7302	−0.011831
9	4.35816	4.38526	−0.621822	55.2104	55.4203	−0.380182
10	7.64194	7.60031	0.544757	3.88654	3.96912	−2.124769

Table 7
Numerical results for $a = 0,\ b = 1,\ f = 0$

n	w_{RK}	w_{IDQ}	Δ%	$\dot{w}_{RK}$	$\dot{w}_{IDQ}$	Δ%
1	0.0000236	0.0000045	80.932203	1.000024334	0.999999999	0.002433
2	0.0000471	0.0000091	80.679406	1.000048565	0.999999997	0.004857
3	0.0000707	0.0000137	80.622348	1.000074082	0.999999992	0.007408
4	0.0000942	0.0000182	80.679406	1.000099548	0.999999986	0.009955
5	0.0001177	0.0000228	80.628717	1.000124962	0.999999979	0.012497
6	0.0001413	0.0000273	80.679406	1.000150322	0.999999969	0.015033
7	0.0001648	0.0000319	80.643204	1.000175628	0.999999945	0.017565
8	0.0001883	0.0000365	80.616038	1.00020088	0.999999945	0.020089
9	0.0002119	0.000041	80.651251	1.000226078	0.999999931	0.022610
10	0.0002354	0.0000456	80.628717	1.000251222	0.999999914	0.025124

Table 8
Numerical results for $a = 0,\ b = 1,\ f = 100$

n	w_{RK}	w_{IDQ}	Δ%	$\dot{w}_{RK}$	$\dot{w}_{IDQ}$	Δ%
1	0.186743	0.187593	−0.455171	32.837344	32.816316	0.064037
2	2.470142	2.49221	−0.893390	60.280012	60.314796	−0.057704
3	7.346964	7.337066	0.134722	33.749065	34.023062	−0.811865
4	5.950286	5.97165	−0.359042	−53.849007	−54.204098	−0.659420
5	1.361149	1.367013	−0.430812	−53.611221	−53.518517	0.172919
6	0.039388	0.041041	−4.196710	−22.84151	−22.753269	0.386319
7	−0.00195	0.000351	118.000000	8.856387	8.931303	−0.845898
8	0.440679	0.448951	−1.877103	40.738099	40.779598	−0.101868
9	3.619322	3.665857	−1.285738	62.481324	62.59005	−0.174014
10	7.926877	7.885604	0.520672	10.032676	9.8182	2.137775

Table 9
Numerical results for $a = 2,\ b = 0,\ f = 0$

n	w_{RK}	w_{IDQ}	Δ%	$\dot{w}_{RK}$	$\dot{w}_{IDQ}$	Δ%
1	1.991038	1.991173	−0.006780	−1.923257	−1.934688	−0.594356
2	1.964129	1.964746	−0.031413	−3.82817	−3.850904	−0.593861
3	1.919538	1.920889	−0.070382	−5.6962	−5.730289	−0.598452
4	1.857682	1.859897	−0.119235	−7.509574	−7.554749	−0.601565
5	1.779157	1.782209	−0.171542	−9.251316	−9.306661	−0.598239
6	1.684711	1.688426	−0.220513	−10.905176	−10.969159	−0.586721
7	1.575233	1.579324	−0.259708	−12.456823	−12.526452	−0.558963
8	1.45174	1.455859	−0.283728	−13.89219	−13.96418	−0.518205
9	1.315378	1.319162	−0.287674	−15.199977	−15.269711	−0.458777
10	1.167396	1.17052	−0.267604	−16.368769	−16.432365	−0.388520

Table 10
Numerical results for $a=2,\ b=0,\ f=100$

n	w_{RK}	w_{IDQ}	Δ%	$\dot{w}_{RK}$	$\dot{w}_{IDQ}$	Δ%
1	2.222116	2.221304	0.036542	28.998172	29.014682	−0.056935
2	4.019657	4.022992	−0.082967	46.744973	46.964882	−0.470444
3	6.988068	6.953169	0.499408	19.330904	19.858246	−2.727974
4	5.942563	5.972073	−0.496587	−38.754304	−38.760169	−0.015134
5	2.998189	3.025898	−0.924191	−42.304564	−42.618572	−0.742256
6	2.044295	2.047638	−0.163528	−17.663857	−18.027672	−2.059658
7	2.015769	2.01525	0.025747	12.268842	11.892034	3.071260
8	2.671888	2.653541	0.686668	38.778075	38.569615	0.537572
9	5.338567	5.295059	0.814975	43.643802	44.249267	−1.387287
10	7.211664	7.188159	0.325930	−7.580665	−6.353716	16.185242

Table 11
Numerical results for $a=0,\ b=2,\ f=0$

n	w_{RK}	w_{IDQ}	Δ%	$\dot{w}_{RK}$	$\dot{w}_{IDQ}$	Δ%
1	0.000192	0.0001557	18.906250	2.00005	1.9999994	0.002530
2	0.000385	0.0003114	19.116883	2.00009	1.9999977	0.004615
3	0.000578	0.0004671	19.186851	2.00014	1.9999948	0.007259
4	0.00077	0.0006228	19.116883	2.00019	1.9999908	0.009959
5	0.000963	0.0007785	19.158879	2.00023	1.9999856	0.012219
6	0.001155	0.0009342	19.116883	2.00027	1.9999793	0.014533
7	0.001348	0.00109	19.139466	2.00031	1.9997179	0.029600
8	0.001541	0.001246	19.143413	2.00035	1.9999631	0.019342
9	0.001733	0.001401	19.157530	2.00038	1.999953	0.021346
10	0.001926	0.001557	19.158879	2.00042	1.999942	0.023895

Table 12
Numerical results for $a=0,\ b=2,\ f=100$

n	w_{RK}	w_{IDQ}	Δ%	$\dot{w}_{RK}$	$\dot{w}_{IDQ}$	Δ%
1	0.211153	0.212175	−0.484009	33.8509	33.8287	0.065582
2	2.60448	2.62793	−0.900372	60.7507	60.7944	−0.071933
3	7.45309	7.43793	0.203406	31.0367	31.2979	−0.841584
4	5.78497	5.80812	−0.400175	−55.1844	−55.5258	−0.618653
5	1.27095	1.27601	−0.398127	−52.7786	−52.6812	0.184544
6	0.032068	0.0336	−4.777348	−21.8292	−21.7408	0.404962
7	−0.001587	0.000547	134.467549	9.85887	9.93456	−0.767735
8	0.485147	0.493887	−1.801516	41.7283	41.7695	−0.098734
9	3.77979	3.82785	−1.271499	62.4707	62.5866	−0.185527
10	7.95495	7.9109	0.553743	6.72716	6.45692	4.017148

Table 13
Numerical results for $a=1,\ b=1,\ f=0$

n	w_{RK}	w_{IDQ}	$\Delta\%$	$\dot{w}_{RK}$	$\dot{w}_{IDQ}$	$\Delta\%$
1	1.00214	1.00205	0.008981	0.759509	0.759686	−0.023305
2	1.00371	1.00354	0.016937	0.51855	0.518939	−0.075017
3	1.00469	1.00447	0.021897	0.277231	0.277895	−0.239511
4	1.00509	1.00483	0.025868	0.03571	0.036693	−2.752730
5	1.00491	1.00464	0.026868	−0.205865	−0.20453	0.648483
6	1.00415	1.003881	0.026789	−0.447306	−0.445636	0.373346
7	1.00281	1.00256	0.024930	−0.688501	−0.686488	0.292374
8	1.00089	1.00068	0.020981	−0.929314	−0.926948	0.254596
9	0.998382	0.998243	0.013923	−1.16964	−1.16688	0.235970
10	0.995304	0.995244	0.006028	−1.40929	−1.40614	0.223517

Table 14
Numerical results for $a=1,\ b=1,\ f=100$

n	w_{RK}	w_{IDQ}	$\Delta\%$	$\dot{w}_{RK}$	$\dot{w}_{IDQ}$	$\Delta\%$
1	1.18911	1.19038	−0.106803	31.9161	31.9185	−0.007520
2	3.2703	3.29077	−0.625936	54.7462	54.8883	−0.259561
3	7.23199	7.21074	0.293833	26.2575	26.5268	−1.025612
4	5.93497	5.9551	−0.339176	−47.257	−47.5317	−0.581290
5	2.14339	2.15529	−0.555195	−48.7839	−48.8414	−0.117867
6	1.03081	1.03234	−0.148427	−20.791	−20.7951	−0.019720
7	1.00012	1.00146	−0.133984	10.5493	10.5411	0.077730
8	1.50829	1.51336	−0.336142	40.5958	40.6034	−0.018721
9	4.49512	4.52249	−0.608883	54.949	55.1705	−0.403101
10	7.64978	7.60784	0.548251	1.10743	1.15721	−4.495092

Table 15
Numerical results for $a=2,\ b=2,\ f=0$

n	w_{RK}	w_{IDQ}	$\Delta\%$	$\dot{w}_{RK}$	$\dot{w}_{IDQ}$	$\Delta\%$
1	2.009742	2.009384	0.017813	0.048664	0.037851	22.219711
2	2.001015	2.000696	0.015942	−1.903421	−1.924665	−1.116096
3	1.973902	1.973991	−0.004509	−3.836878	−3.868446	−0.822752
4	1.928669	1.929444	−0.040183	−5.732591	−5.774507	−0.731188
5	1.865754	1.867361	−0.086131	−7.57228	−7.62414	−0.684866
6	1.785773	1.788198	−0.135796	−9.338095	−9.399136	−0.653677
7	1.689498	1.69258	−0.182421	−11.013757	−11.082085	−0.620388
8	1.577858	1.581315	−0.219094	−12.583729	−12.656714	−0.579995
9	1.45191	1.455399	−0.240304	−14.034513	−14.108257	−0.525448
10	1.312849	1.316009	−0.240698	−15.353275	−15.423771	−0.459159

Table 16
Numerical results for $a = 2,\ b = 2,\ f = 100$

n	w_{RK}	w_{IDQ}	Δ%	$\dot{w}_{RK}$	$\dot{w}_{IDQ}$	Δ%
1	2.272414	2.27165	0.033621	30.71655	30.738601	−0.071789
2	4.218993	4.222418	−0.081181	46.861133	47.10417	−0.518632
3	7.090236	7.052999	0.525187	15.250495	15.770967	−3.412820
4	5.729613	5.764015	−0.600424	−40.792579	−40.838435	−0.112413
5	2.871101	2.896194	−0.873985	−41.12235	−41.441702	−0.776590
6	2.031366	2.034074	−0.133309	−15.741702	−16.108022	−2.327067
7	2.023462	2.022358	0.054560	14.220838	13.847342	2.626399
8	2.779282	2.759136	0.724863	40.127061	39.946119	0.450923
9	5.55926	5.513668	0.820109	42.167826	42.856437	−1.633025
10	7.153621	7.140019	0.190141	−11.941588	−10.777357	9.749382

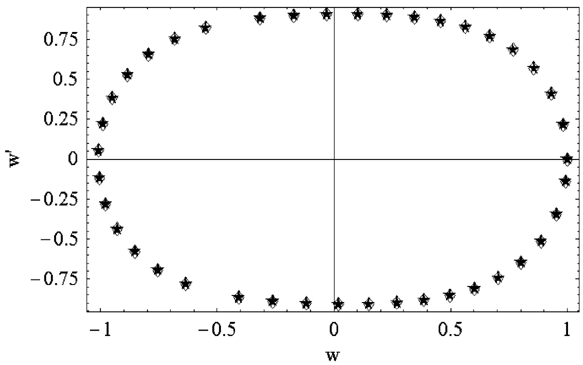

Fig. 1. Poincaré map for $f = 0.01$ (40 points): ◇, Runge–Kutta results; ★, IDQ results.

The percentage difference of the IDQ solution with regard to the Runge–Kutta results is obtained as

$$\Delta = \frac{w_{RK} - w_{IDQ}}{w_{RK}} \times 100,$$

where *RK* stands for Runge–Kutta.

The tables show a noticeable difference with the Runge–Kutta results for cases with the initial displacement equal to zero. This difference is limited to the displacements and decreases with increasing n and disappears more quickly by increasing the initial velocity and the amplitude of the forcing term. In any case, differences between the results shown in the tables do not diverge.

Sign inversions may affect solutions closest to zero, as in Tables 8 and 12.

The long-term solution will be discussed in the next section.

All the computations have been made by means of a *Mathematica* package created by the author.

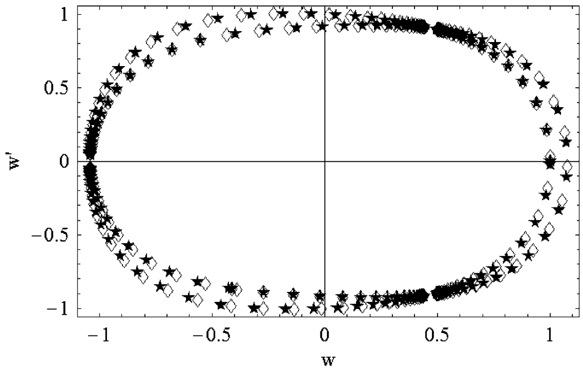

Fig. 2. Poincaré map for $f = 0.023$ (214 points): ◇, Runge–Kutta results; ★, IDQ results.

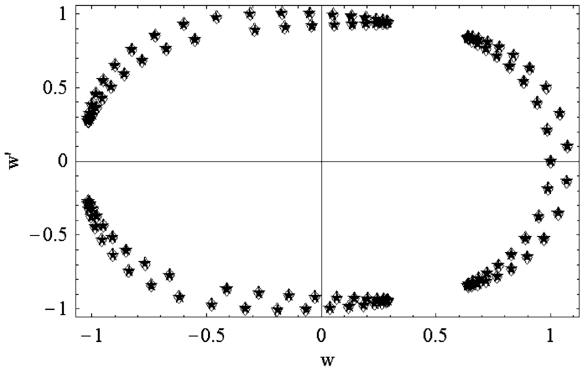

Fig. 3. Poincaré map for $f = 0.025$ (120 points): ◇, Runge–Kutta results; ★, IDQ results.

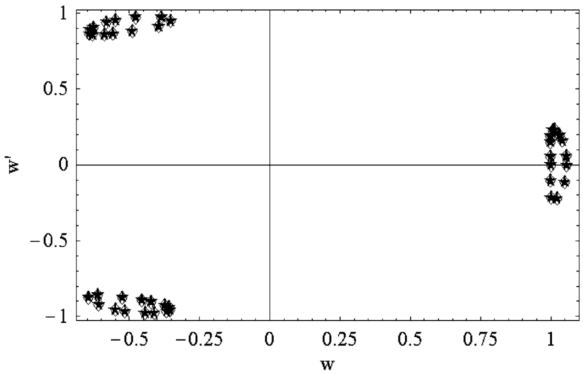

Fig. 4. Poincaré map for $f = 0.2$ (40 points): ◇, Runge–Kutta results; ★, IDQ results.

6. Simulations

Two examples have been considered. Attention is drawn to the first oscillator. As already stated in the previous section, $\Delta\tau = T/4$ has been assumed, where T has the meaning explained above.

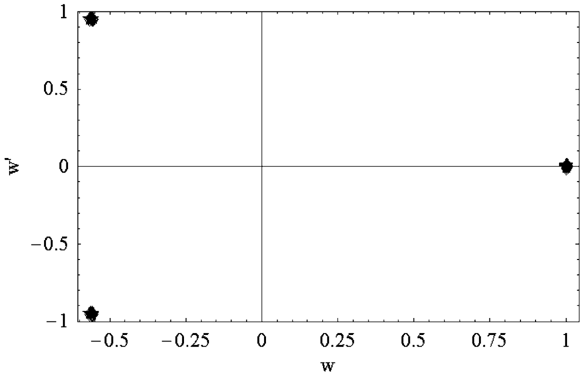

Fig. 5. Poincaré map for $f = 0.6$ (20 points): ◇, Runge–Kutta results; ★, IDQ results.

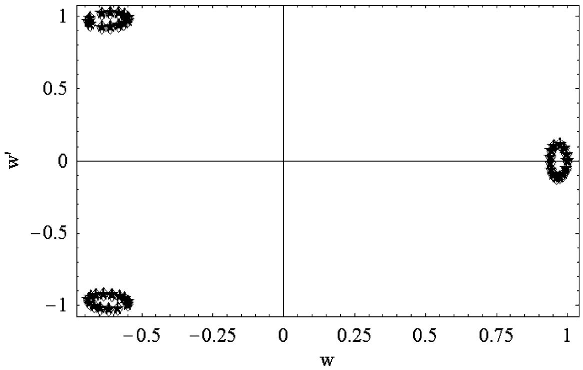

Fig. 6. Poincaré map for $f = 1$ (40 points): ◇, Runge–Kutta results, ★, IDQ results.

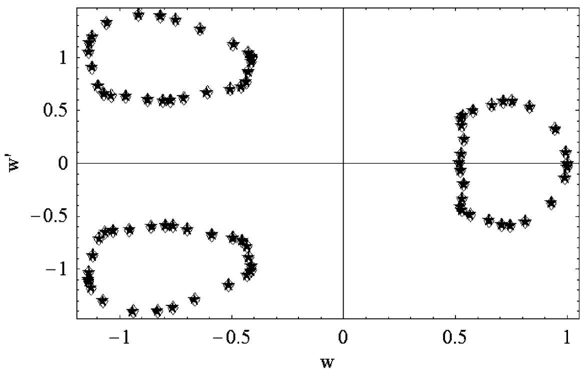

Fig. 7. Poincaré map for $f = 2.5$ (80 points): ◇, Runge–Kutta results; ★, IDQ results.

6.1. First example

Firstly, the case with the first natural frequency closest to zero (or equal to zero with regard to the Galerkin solution) has been considered. So, $\sigma = \pi^2$ and $\theta_1 = 0$ has been chosen. In addition,

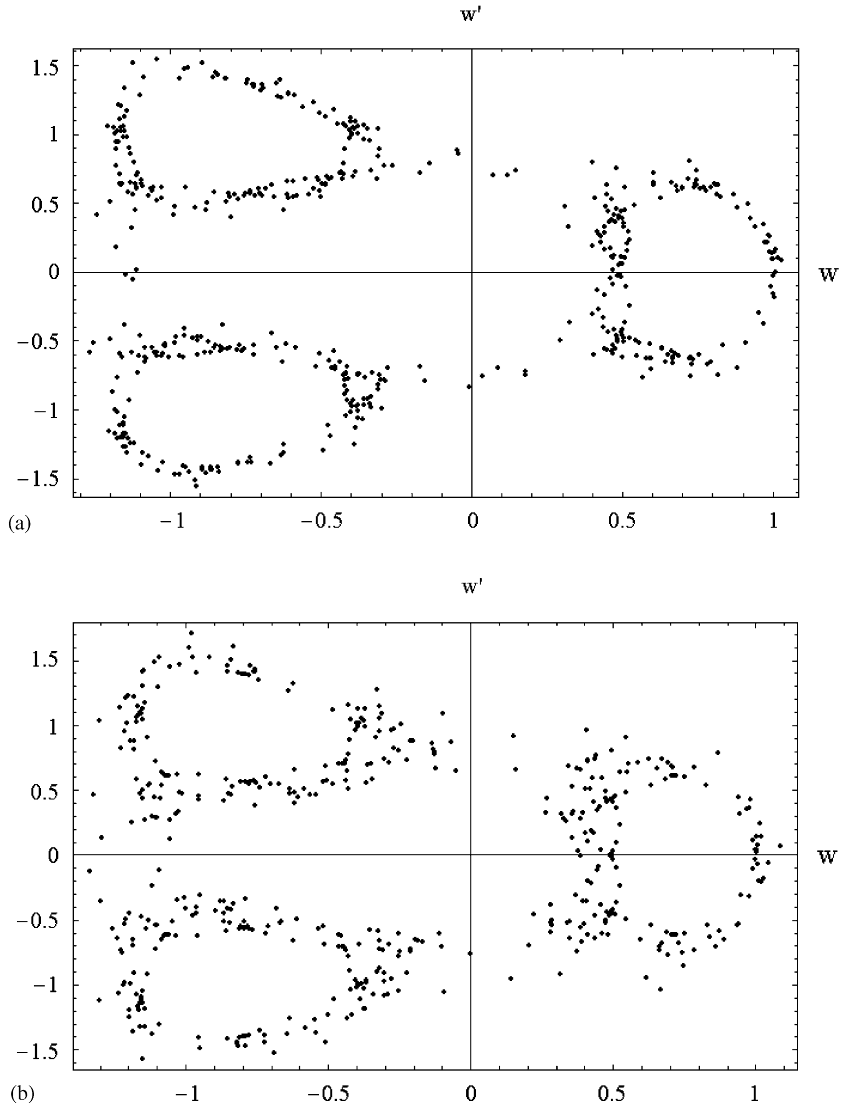

Fig. 8. Poincaré map for $f = 2.55$ (500 points): (a) Runge–Kutta method, (b) IDQ method.

$\theta_3 = 1$ and $\omega = \pi$ have been fixed. The behaviour of the resulting system has been studied by drawing Poincaré maps with a large number of points. A Poincaré map, a stroboscopic motion of the trajectory on a section plane in the phase space, is a common way of displaying the dynamics of almost-periodic motion, as in the case considered.

In order to visualize a comparison between points obtained with the IDQ method and those obtained with the Runge–Kutta method, the number of points has been limited were as far as possible without losing the shape of curves on the Poincaré section. Figure captions indicate the number of points which has been used to draw the map.

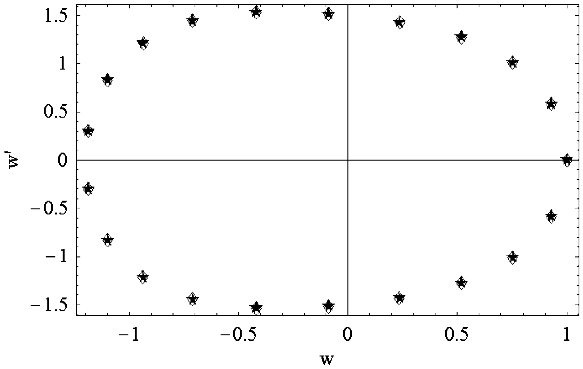

Fig. 9. Poincaré map for $f = 1$ (20 points): ◇, Runge–Kutta results; ★, IDQ results.

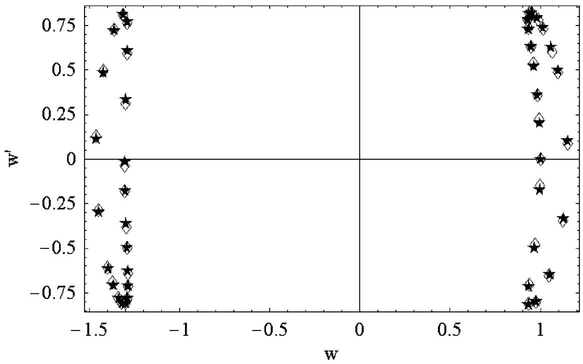

Fig. 10. Poincaré map for $f = 1.5$ (40 points): ◇, Runge–Kutta results; ★, IDQ results.

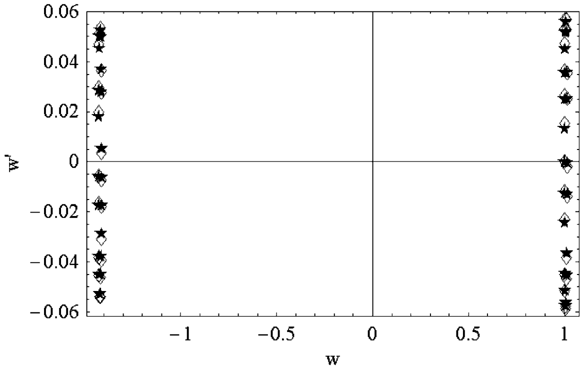

Fig. 11. Poincaré map for $f = 2$ (40 points): ◇, Runge–Kutta results; ★, IDQ results.

On the Poincaré section, a two-frequency almost-periodic motion is represented by a closed loop. This can be seen in Fig. 1 for the amplitude of the forcing term $f = 0.01$.

The transition from a motion on a torus to a motion on a two-torus is pointed out in Fig. 2 for $f = 0.023$, even if the limited number of points does not display correctly the continuity of loops. With a small increase of the amplitude of the forcing term, i.e., for $f = 0.023285$, a breakdown in

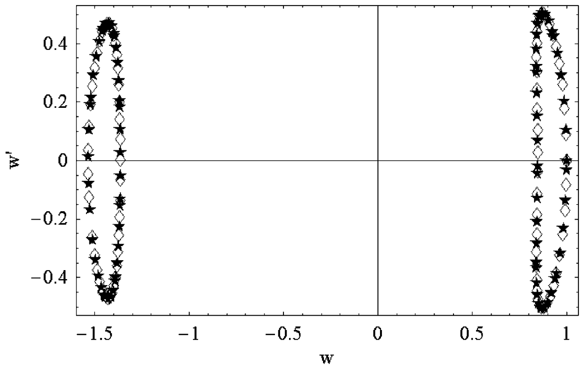

Fig. 12. Poincaré map for $f = 2.5$ (80 points): ◇, Runge–Kutta results; ★, IDQ results.

the continuity of loops occurs. This could be due to an exterior crisis, which is the sudden destruction of a chaotic attractor, caused by the collision of the chaotic attractor with an unstable orbit or with its invariant manifolds at its boundary of basin of attraction.

So, on the Poincaré section, one can see three closed loops, whose dimension decreases by increasing the amplitude of the forcing term until $f = 0.6$ (Figs. 3–5). In particular, for $f = 0.63$ one can see three points on the map corresponding to a $3T$-periodic motion, where T is the period of the forcing term. For values of f greater than 0.6, the dimension of the closed loops increases until $f = 2.5$ (Figs. 6 and 7). At $f = 2.55$, chaos appears suddenly (Fig. 8).

All the figures show a good agreement between IDQ results and Runge–Kutta results. Even if there may be some differences between points, the Poincaré maps are preserved, as confirmed in Fig. 8, where an indirect comparison between points has been forced by a greater number of points.

6.2. *Second example*

First, natural frequency closest to the unit (or equal to the unit with regard to the Galerkin solution) has been assumed. So, $\sigma = \pi^2$ and $\theta_1 = 1$ has been chosen. Besides, $\theta_3 = 1$ and $\omega = \pi$.

Fig. 9 shows an almost-periodic motion on a torus for $f = 1$. By increasing the amplitude of the forcing term, on the Poincaré section, two closed loops appear (Fig. 10), whose dimension decreases until $f = 2$ (Fig. 11). For values of f greater than 2 the dimension of the closed loops increases (Fig. 12).

For $f = 2.99$ (Fig. 13), a behaviour is observed which seems to denounce a crisis-induced intermittency, which occurs when the chaotic attractor collides with a periodic orbit in the interior of its basin.

All the figures again show good agreement between IDQ results and Runge–Kutta results.

7. Conclusions

In this paper, an iterative method based on differential quadrature rules has been proposed. Computer experiments on dynamical systems allowed one to choose appropriate values of the

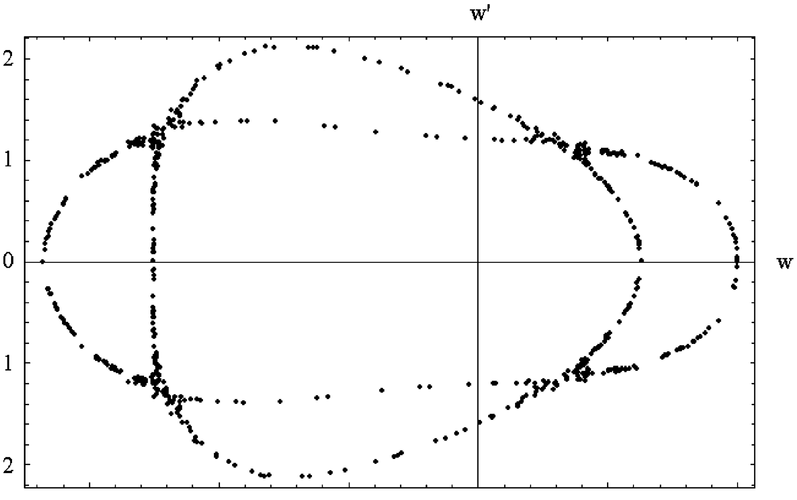

(a)

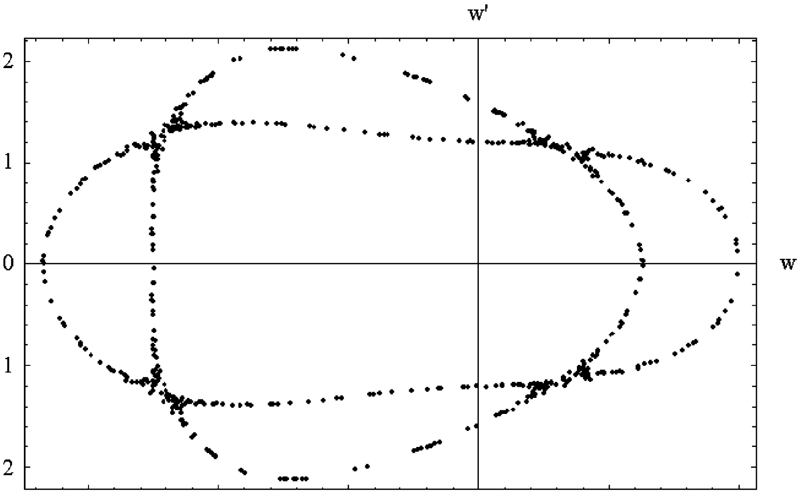

(b)

Fig. 13. Poincaré map for $f = 2.99$ (600 points): (a) Runge–Kutta method, (b) IDQ method.

parameters which influence the solution in the space–time domain. These parameters are the distribution of the sampling points and the length of the time interval.

A rule for generating sampling points, already used to discretize the space domain, has been successfully used to discretize the whole space–time domain. In fact, the distribution of sampling points obtained by this rule is repeated in each of the intervals which compose the discretized time domain. In this way, it is possible to use only one distribution to solve dynamical problems.

By applying quadrature rules, the non-linear partial differential equation reduces to a set of non-linear algebraic equations, which can be solved with Newton's method.

As an example, a simple structural model has been investigated by using the IDQ method and Runge–Kutta method, in particular, to draw Poincaré maps. Numerical results show that the proposed method behaves quite satisfactorily.

Acknowledgements

The author acknowledges Professor Claudio Franciosi for helpful discussion about non-linear dynamical systems.

References

[1] S. Tomasiello, Differential quadrature method: application to initial-boundary-value problems, Journal of Sound and Vibration 218 (4) (1998) 573–585.
[2] A.Y.T. Leung, S.K. Chui, Non-linear vibration of coupled Duffing oscillators by an improved incremental harmonic balance method, Journal of Sound and Vibration 181 (4) (1995) 619–633.
[3] K. Yagasaki, T. Ichikawa, Higher-order averaging for periodically forced, weakly nonlinear oscillators, International Journal of Bifurcation and Chaos 9 (1999) 519–531.
[4] K. Yagasaki, Numerical detection and continuation of homoclinic points and their bifurcations for maps and periodically forced systems, International Journal of Bifurcation and Chaos 8 (1998) 131–148.
[5] C.W. Bert, M. Malik, Differential quadrature method in computational mechanics: a review, Applied Mechanic Review 49 (1) (1996) 1–28.
[6] T.Y. Wu, G.R. Liu, The generalized differential quadrature rule for initial-value differential equations, Journal of Sound and Vibration 233 (2) (2000) 195–213.
[7] G.R. Liu, T.Y. Wu, An application of the generalized differential quadrature rule in Blasius and Onsager equations, International Journal for Numerical Methods in Engineering 52 (2001) 1013–1027.
[8] T.Y. Wu, G.R. Liu, Application of the generalized differential quadrature rule to eigth-order differential equations, Communications in Numerical Methods in Engineering 17 (5) (2001) 355–364.
[9] T.Y. Wu, G.R. Liu, Free vibration analysis of circular plates with variable thickness by the generalized differential quadrature rule, International Journal of Solids and Structures 38 (2001) 7967–7980.
[10] G.R. Liu, T.Y. Wu, Numerical solution for differential equations of Duffing-type non-linearity using the generalized differential quadrature rule, Journal of Sound and Vibration 237 (5) (2000) 805–817.
[11] C. Shu, H. Du, Implementation of clamped and simply supported boundary conditions in the GDQ free vibration analysis of beams and plates, International Journal of Solids and Structures 34 (7) (1997) 819–835.